

Evaluation of a 16:3 Signal Multiplexor to Acquire Signals From a SPM Array With Dual and Single Layer LYSO Crystal Blocks

Christopher J. Thompson, *Senior Member, IEEE*, and Andrew L Goertzen, *Member, IEEE*

Abstract—For many years most PET scanners have used a large number of crystals with some form of light sharing technique to couple them to four photo-multiplier tubes (PMT). While the resolution of the scanners was improved by using a larger number of smaller crystals, the PMT size had remained about the same since it is not practical to make PMTs very small. Avalanche photo-diodes (APD) and silicon photo-multipliers (SPM) are now replacing PMTs in small animal PET scanners and in MR-PET scanners in which PMTs are not practical due to their sensitivity to magnetic fields. In this paper we study the performance of a dual layer PET detector consisting a 4×4 array of $3.3 \text{ mm} \times 3.3 \text{ mm}$ LYSO crystals in the lower layer and an upper offset layer of 3×3 crystals coupled to a SensL SPMArray4 4×4 array of SPMs. A single layer array of $1.68 \text{ mm} \times 1.68 \text{ mm}$ crystals is also studied. The standard SensL pre-amplifier and evaluation board were used to process the signals. The 16 outputs of the evaluation board were connected directly to 16 ADC channels or through a 16:3 multiplexor which uses simple summing amplifiers to provide bipolar X and Y signals as well as the sum of all inputs. In this case only 3 ADCs are required to encode the signals. In both cases a crystal identification map is produced in software. The use of the multiplexor has a negligible effect on the size of each crystal's foot-print or its energy resolution. We introduce the concept of "resolvability index" (RI) to compare the size of each crystal's foot-print and distance to its neighbour. Our results suggest that the RI with the multiplexed SPM readout is comparable to that of a conventional PS-PMT readout, and superior to that of conventional PET detectors with four PMTs. We anticipate that even smaller crystals could be used on the SPM making this a good choice for small animal PET scanners.

Index Terms—Block detector, multiplexed output, PET, silicon photomultiplier.

I. INTRODUCTION

FOR many years most PET scanners have used a large number of crystals with some form of light sharing technique to couple them to four photo-multipliers (PMT). While the resolution of the scanners was improved by using a larger number of smaller crystals, the PMT size had remained about

Manuscript received January 18, 2011; revised April 01, 2011; accepted May 23, 2011. This work was supported by grants from the Natural Science and Engineering Research Council of Canada to Dr. Thompson (OGP-0036672) and Dr. Goertzen (341628-2007) and a Manitoba Health Research Council operating grant to Dr. Goertzen. The data from the Siemens Inveon detector was acquired by Bryan McIntosh, student of ALG.

C. J. Thompson is with the Montreal Neurological Institute, McGill University, Montreal, QC H4J 1X8 Canada (e-mail: Christopher.Thompson@McGill.Ca).

A. L. Goertzen is with the Department of Radiology, University of Manitoba, Winnipeg, MB R3E 3P4 Canada (e-mail: GoertzeA@cc.UManitoba.Ca)

Color versions of one or more of the figures in this paper are available online at <http://ieeexplore.ieee.org>.

Digital Object Identifier 10.1109/TNS.2011.2160202

the same since it is not practical to make PMTs very small. Apart from the pioneering work of Roger Lecomte [1] and others it was not until recently that developers of PET scanners have seriously considered solid state imaging systems such as avalanche photo-diodes (APD) and silicon photo-multipliers [2] (SPM). This development is in part due to the advent of magnetic resonance imaging compatible MR-PET scanners [3] in which PMTs are not practical due to their sensitivity to magnetic fields but also due to the limited number of manufacturers still making PMTs. The so-called PET "block detectors" have between 16 and 169 crystals on four PMTs [4], so that only four signal leads and amplifiers are required to process events from a large number of crystals resulting in a relatively simple processing stream. Solid state light sensors are normally quite small, have less gain than PMTs and thus require more signal leads and amplifiers than PMTs. Since sophisticated crystal mapping software has been developed for use with block detectors, it seems logical to use some sort of multiplexing of solid state photo detector arrays to simplify the wiring of PET scanners in order to reduce their cost, complexity, and maintenance.

In this paper we propose a multiplexing scheme for the 16 outputs of the SensL SPM-4 array of silicon photo-multipliers. Rather than multiplex the rows and columns with capacitors as has been demonstrated by the Stanford group [5] (reducing the number of leads from 16 to four), we propose a set of three simple resistive mode summing amplifiers which provide a sum of all signals for an energy output, E, and bi-polar signals which provide the raw X and Y coordinates for the crystal map. We demonstrate the performance of this multiplexor and compare it with a simple 1:1 coupling and 16 ADCs to provide a crystal identification map in a dual layer LYSO crystal array. We anticipate that the multiplexor could be constructed as a simple integrated circuit since it does not need any matched capacitors. The three signals could be digitized using a three input ADC similar to those used to digitize colour TV signals. A fixed reference voltage would be used for digitizing the energy signal. The sum or energy signal would become the reference for the X and Y so as to provide bipolar X/E and Y/E crystal mapping coordinates.

II. MATERIALS AND METHODS

A. Description of Crystal Arrays

Dual layer crystal arrays were constructed using polished LYSO crystals supplied by a commercial producer (Proteus

Inc., Chagrin Falls, OH). Sixteen 13.5 mm × 3.3 mm × 3.3 mm crystals were arranged in a 4 × 4 array in the bottom layer and nine 6.5 mm × 3.3 mm × 3.3 mm crystals were arranged in a 3 × 3 array in the upper layer. The crystals were separated with white Toray film cut in a pattern similar to that made in cardboard to separate bottles in a packing box. The layers were glued together with double sided transparent sticky pads and mounted on the SPMArray4 array. The crystals were directly coupled to the sensors with optical grease.

Another commercially available LYSO array manufactured by Agile Engineering, Knoxville, TN, was also used. It had 1.68 mm × 1.68 mm × 10 mm crystals in an 11 × 11 array. The crystals are glued together with reflective optical barriers between the crystals forming a solid block 18.5 mm × 18.5 mm square. This array is too big to fit on the sensor so one edge was lined up and the array was otherwise symmetrically placed on the sensor array.

In both cases, the detectors were placed in a light tight metal box along with the pre-amplifier supplied with the SPM array (see Section II-B). A 50-way flat ribbon cable connects the box to a SensL evaluation board which provides a sum signal and 16 individual SMA connectors. Cables from these connectors route signals from the evaluation board to either the multiplexor or directly to a traditional shaping amplifier and three Jorway six input ADCs. One single detector was tested by exposing it to a Scanwell timing alignment probe [6] with a ²²Na source.

B. Sensor and Pre-Amplifier

The instrumentation is based on a SensL [7] SPMArray-4 16 silicon photomultiplier array, a SensL SPMArray -A0 pre-amplifier into which the sensor array installs and a SensL SPMArray -A1 evaluation board. The evaluation board receives signals from the sensors, sums them to provide a timing trigger, and allows the data acquisition system to be connected via SMA coaxial connectors. The gain of the sum channel was reduced 40% by adding a 330 Ω resistor in parallel with the 470 Ω feedback resistor in order to prevent the output saturating when using LYSO crystals and the manufacturer's recommended bias. Previous studies [8] showed that there was little change in energy and timing resolution with bias voltage, although the pulse height changes linearly with bias voltage above the threshold. A BK Precision Model 1550 digitally regulated variable precision power supply was used to adjust the SPM bias to match the shaping amplifier and multiplexor inputs and ADC voltage range.

C. Multiplexor

In order to reduce the number of acquisition channels required a novel multiplexor-shaping amplifier was designed and built at Niagara Engineering Works, Winnipeg Manitoba. This device has 16 BNC inputs to receive the signals from the evaluation board. The inputs of each channel are terminated in 50 Ω and buffered by unity gain AD-9631 operational amplifiers. The four weighting stages are implemented with AD-8620 operational amplifiers with time constants of 300 nsec. Additional amplifiers are used to compute the difference of two X values and two Y values. This delays the output slightly. The summing

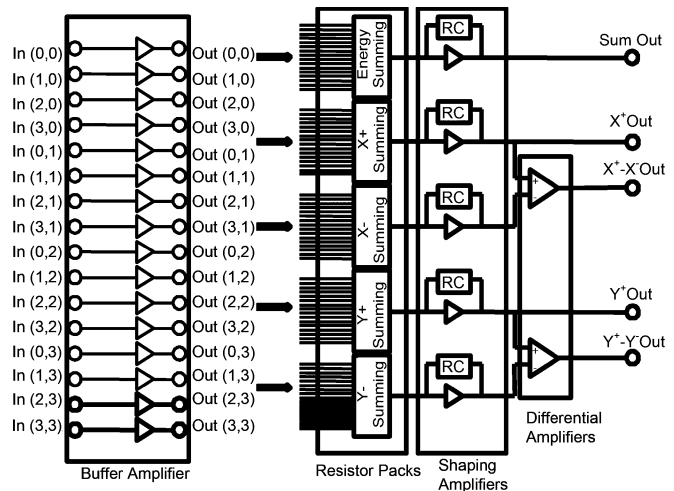


Fig. 1. Conceptual schematic of multiplexor showing the buffer amplifiers at the inputs, and five resistor packs allowing various weighting schemes to be tested.

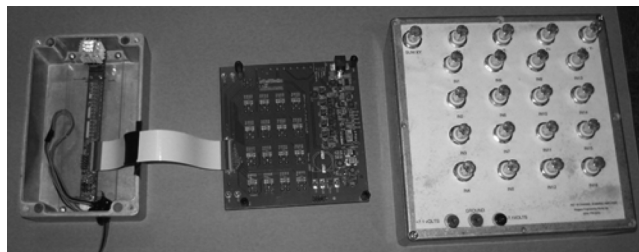


Fig. 2. SensL detector with dual-layer crystal in light-tight box, SensL evaluation board, and 16:3 multiplexor.

stage also uses an AD-8620 but with a 500 nsec time constant to delay its output so that the peak of all three signals occurs at the same time for input to the ADC. The circuit board has five 16-component sockets which can be filled with resistors between the buffered inputs and the common negative input of the operational amplifiers. Various resistors can be inserted in these to establish the arithmetic function desired. One is used as a simple sum with equal resistors, the others have only 1/2 of the resistor positions used in order to provide an X+, X-, Y+ and Y- signal. The X outputs are then subtracted as are the Y outputs producing bipolar outputs weighted by the sensor element's distance from the centre of the array. A conceptual circuit diagram is presented in Fig. 1. A photograph of the detector, SensL evaluation board and multiplexor is presented in Fig. 2. The multiplexor/shaping amplifier uses various resistors to be used to establish the optimal weighting scheme for generating the crystal map. In the studies reported here the value of the weighting resistors for the outer rows and columns was 1/3 of the central ones to provide three times more gain for the outer elements. In these studies the sum resistors were all 1000 Ω and the weighting resistors were either 330 Ω or 1000 Ω giving gain ratios of 3:1 for the outer and inner crystals according to the standard form of the operation amplifier gain equation viz:

$$V_{out} = V_{in} \frac{R_f}{R_{in}} \quad (1)$$

The weighting values (R_f/R_{in}) for each sensor element are shown in (2) according to their rows and columns.

$$\begin{aligned}
 E &= \begin{bmatrix} 1 & 1 & 1 & 1 \\ 1 & 1 & 1 & 1 \\ 1 & 1 & 1 & 1 \\ 1 & 1 & 1 & 1 \end{bmatrix} \\
 Y &= \begin{bmatrix} 3 & 3 & 3 & 3 \\ 1 & 1 & 1 & 1 \\ 0 & 0 & 0 & 0 \\ 0 & 0 & 0 & 0 \end{bmatrix} - \begin{bmatrix} 0 & 0 & 0 & 0 \\ 0 & 0 & 0 & 0 \\ 1 & 1 & 1 & 1 \\ 3 & 3 & 3 & 3 \end{bmatrix} \\
 X &= \begin{bmatrix} 0 & 0 & 1 & 3 \\ 0 & 0 & 1 & 3 \\ 0 & 0 & 1 & 3 \\ 0 & 0 & 1 & 3 \end{bmatrix} - \begin{bmatrix} 3 & 1 & 0 & 0 \\ 3 & 1 & 0 & 0 \\ 3 & 1 & 0 & 0 \\ 3 & 1 & 0 & 0 \end{bmatrix} \quad (2)
 \end{aligned}$$

D. Data Acquisition and Display and Analysis Software

The signals from the SensL evaluation board were either processed by conventional shaping amplifiers in a 16 channel NIM module, or by the multiplexor. The fast sum output of the SensL board is connected to a Canberra Model 454 constant fraction discriminator (CFD) the output of which is delayed to trigger either one or four CAMAC Jorway Aurora-14 six channel ADCs at the peak of the multiplexor outputs. The CAMAC crate is interfaced to a VAXstation 4000/90 workstation which has been programmed to acquire and display the data. The programs allow for the acquisition of 16 channels from the array or three from the multiplexor. Data is collected in “list mode” and other very similar programs allow for the playback with different discriminator settings or crystal map. Another program is used to manually identify the regions of the crystal image corresponding to each crystal. This program produces a crystal map file which identifies the specific crystal (X, Y, Z in the block) associated with that region. This is then used to correct for the gain of each crystal by scaling the discriminator settings for that specific crystal.

An extensive display and analysis program allows the display of the data, with windows in which regions of interest are defined and analysed, and profiles can be drawn. Since the crystal images from PET detectors are often distorted, profiles can be drawn by pointing to the peaks of individual crystals, so that the line on the image joins the crystal dots, but the profile through that line is displayed. These so called “dot-join” profiles are displayed beside the images as coloured lines corresponding to the line drawn on the image. The values of each point in the profile are exported in order to estimate the performance of the imaging system. The exported profiles are analysed by another program. This program calculates the FWHM and FWTM of peaks from each crystal in the profile by fitting points from each peak as measured above the neighbouring valley floors to the sum of three Gaussian curves using the Levenberg- Marquardt [9] technique.

We report the performance of each method in terms of a “resolvability index” [10], RI which we define as:

$$RI = \frac{FWHM}{D} \quad (3)$$

where D is the distance separating each crystal’s centre, and FWHM is the full width at half maximum of one segment of a profile through the 2D histogram of events in which a γ -ray interacted with a row of crystals. Classically. Two objects are considered resolved when the FWHM is less than the peak separation, (ie $RI < 1.0$). Thus, for smaller values of RI, more crystals could be resolved by the same sensor. Compton scatter between crystals creates a series of vertical, horizontal and diagonal lines that appear to connect the crystal blobs in the flood histogram images. These lines reduce the utility of conventional peak-to-valley measurements for estimating crystal resolvability. For comparison with better known PET detector blocks, the RI was measured for detectors from a Siemens Molecular Imaging Biograph HiRez [11] 13×13 crystal block and an Inveon [12] 20×20 crystal block, data from which was acquired in a compatible data acquisition system.

E. Experimental Studies

A Scanwell PET timing alignment probe [6] with a 100 uCi source was placed 15 cm from the detector under test. Acquisitions of 16 channel and three channel multiplexed data were performed at SPM bias voltages of 27.8 to 29.2 volts in 0.2 Volt steps. For the studies presented here the data sets at 28.7 and 28.2 Volts were used as ones which maximised the dynamic range of the amplifiers and ADC. The recommended bias for this SPM was 28.0. Data were acquired as a preset number of counts, and each acquisition took about 5 live-time minutes. Data were acquired for each of the two detector modules, the dual-layer block, and the commercial 1.68 mm crystal block. Acquisitions with both the 16 channel and 16:3 multiplexed configurations were made.

The data were analysed by drawing profiles through the peaks of crystal maps in all cases, and estimating the width of the profiles through the crystal image “blobs” as a measure of the noise present in the entire processing chain. Any difference between the 16-channel and 3-channel acquisitions was assumed to be due to the noise associated with the multiplexor. Spectral photo-peaks were also analysed and their peak position and FWHM measured by fitting the peak to a Gaussian using Graph-Pad Prism.[13]

The resolvability data obtained in these SPM studies is compared with previous experiments in which the same dual-layer crystals were coupled to a Hamamatsu R7600-00 C12 PS-PMT [14] in order compare the RI of the SPM and conventional PS-PMT under identical conditions: same crystal configuration; same data acquisition system.

III. RESULTS

Profiles through the block with two layers of 3.3 mm crystals are shown in Fig. 3; the 16 channel acquisition in Fig. 3 (top), and the 16:3 multiplexed acquisition in Fig. 3 (bottom). The profiles were drawn by connecting the peak of each crystal’s territory alternating from the lower layer to the upper layer. The crystals are 3.3 mm wide so the effective crystal separation in 1.65 mm. These profiles were segmented as explained previously and the results showing the resolution for each crystal are presented in Table I, for both the 16 and 3 channel acquisitions. The average FWHM of the crystal blobs is 0.38 mm for the 16

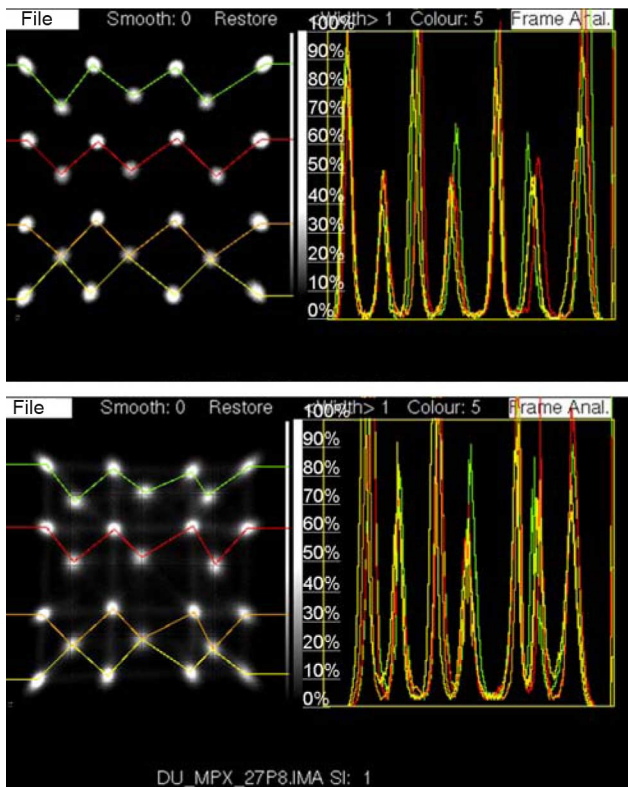


Fig. 3. Top: Profiles through 16 channel acquisition, and Bottom: Profiles through multiplexed acquisition. The profiles are made by pointing to the center of each crystal's region for each row in the dual-layer 3.3 mm crystal array.

TABLE I

RESOLUTION MEASUREMENTS FOR DUAL-LAYER DETECTORS WITH 3.3 MM CRYSTALS FOR BOTH 16 CHANNEL AND 16:3 MULTIPLEXED STUDIES

Row #	16 Individual Channels		16:3 Multiplexed Channels	
	FWHM (mm)	FWTM (mm)	FWHM (mm)	FWTM (mm)
1	0.36±.06	0.70±.09	0.43±.064	0.87±.12
2	0.39±.09	0.78±.17	0.42±.11	0.91±.18
3	0.38±.10	0.71±.19	0.39±.09	0.89±.30
4	0.39±.05	0.75±.09	0.46±.08	1.01±.16
Ave	0.38 ±01	0.74 ±04	0.43 ±01	0.92 ±03

channel acquisitions which degrades to 0.43 mm in the multiplexed study.

Profiles through the block with a single layer of 1.6 mm crystals are shown in Fig. 4; the 16 channel acquisition in Fig. 4 (top), and the 16:3 multiplexed acquisition in Fig. 4 (bottom). The profiles were drawn by connecting the peak of each crystal's territory in each row of crystals. The crystals are 1.6 mm wide so the effective crystal separation in 1.6 mm. These profiles were segmented as explained previously and the results showing the resolution for each crystal are presented in Table II, for both the 16 and 3 channel acquisitions. The average FWHM of the crystal blobs is 0.38 mm for the 16 channel acquisitions which degrades to 0.50 mm in the multiplexed study.

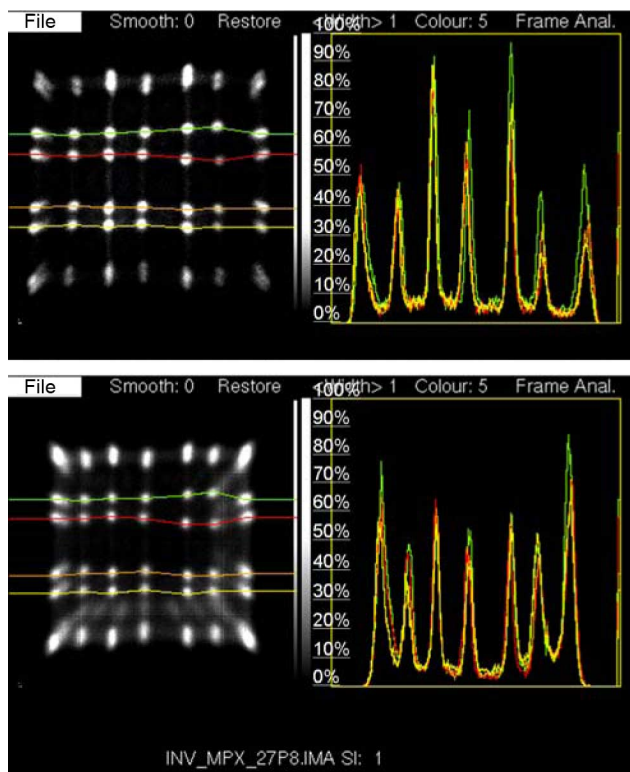


Fig. 4. Top: Profiles through 16 channel acquisition, and Bottom: Profiles through multiplexed acquisition. The profiles are made by pointing to the center of each crystal's region for each row in the single layer 1.6 mm crystal array.

TABLE II

RESOLUTION MEASUREMENTS FOR SINGLE-LAYER DETECTORS WITH 1.6 MM CRYSTALS FOR BOTH 16 CHANNEL AND 16:3 MULTIPLEXED STUDIES

Row #	16 Individual Channels		16:3 Multiplexed Channels	
	FWHM (mm)	FWTM (mm)	FWHM (mm)	FWTM (mm)
2	0.39±.06	0.96±.13	0.52±.15	1.11±.10
3	0.41±.07	0.96±.12	0.49±.08	1.09±.13
4	0.38±.03	1.08±.26	0.51±.06	1.21±.21
5	0.33±.04	1.05±.32	0.48±.05	1.25±.25
Ave	0.38 ±03	1.01 ±06	0.50 ±02	1.17 ±04

These resolution results are summarized in Table III along with the resolvability index for each of the configurations measured in this study. Also included, for comparison, are the resolvability indexes for detectors used in the Siemens HiRez Biograph, and the Siemens Inveon pre-clinical scanner. As can be seen the RI is slightly degraded from 0.25 to 0.28 for the dual layer detector and the multiplexed acquisition, and from 0.25 to 0.31 for the 1.6 mm single layer block. These should be compared to commercial PET scanner's detectors which have their RI values between 0.53 for the HiReZ block, and 0.41 for the Inveon block.

The energy spectra for crystals in the dual layer blocks are presented in Fig. 5; the 16 channel acquisition in Fig. 5 (top), and the 16:3 multiplexed acquisition in Fig. 5 (bottom). Since the

TABLE III

SUMMARY OF RESULTS SHOWING THE RESOLUTION PARAMETERS FOR STUDIES DESCRIBED IN THIS PAPER AND COMPARING THEM WITH THOSE FROM A SIEMENS HIRez DETECTOR AND A DUAL LAYER CRYSTAL ARRAY COUPLED TO A PS-PMT ACQUIRED WITH THE SAME DATA ACQUISITION SYSTEM, AND A DETECTOR FROM A SIEMENS PRE-CLINICAL INVEON SCANNER ACQUIRED BY ONE OF THE AUTHORS (ALG UNPUBLISHED DATA)

Detector Module	Crystal configuration	FWHM	FWTM	Resolvability Index
SensL 4x4 standard 16 channel acquisition	Upper 3x3 & Lower 4x4 3.3 mm	0.38±.06	0.74±.12	0.25±.01
SensL 4x4 MPX 3 channel acquisition	Upper 3x3 & Lower 4x4 3.3 mm	0.43±.08	0.92±.13	0.28±.01
SensL standard 16 channel acquisition	11x11 1.6 mm	0.38±.05	1.01±.24	0.24±.01
SensL 4x4 MPX 3 channel acquisition	11x11 1.6 mm	0.50±.08	1.17±.21	0.31±.02
Other studies				
Siemens HiRez 4 channel acquisition	13x13 4 mm	2.09±.22	3.40±.78	0.53±.02
PS-PMT dual layer 4 channel acquisition	Upper 5x5 & Lower 6x6 3.3 mm	0.33±.07	0.77±.21	0.22±.02
Siemens Inveon 4 channel acquisition	20x20 1.6 mm	0.63±.10	1.23±.22	0.41±.01

IV. DISCUSSION

We have compared the results from two different crystal configurations of PET detectors coupled to a SensL SPM array when the data is acquired with 16 individual channels and when these data are multiplexed from 16 to 3 channels. In all cases there is some loss of resolution: both spatial and spectral. We introduced the concept of “resolvability index”, RI, to compare these results to commercial PET detectors from well known scanners. Our results suggest that the performance of the detectors which we present here ($RI_{ave} = 0.27$) are significantly better than those from a conventional PET whole body scanner which uses four PMTs to encode 169 crystals ($RI = 0.53$), and those from a pre-clinical PET scanner which uses a cross-wire anode PS-PMT to read out 400 crystals ($RI = 0.41$). The dual-layer crystal block used in these studies had previously been coupled to a PS-PMT and read out with the same pre-amplifiers as are employed in the MicroPET Focus pre-clinical scanner. These studies were presented at the 2008 IEEE MIC (Abstract M6-49) [14] but the detailed results were not published at the time. When this configuration is compared with the present study, the RI for the PS-PMT experiment was 0.22 which is only slightly better than the values of 0.25 and 0.28 from the 16 channel and MPX acquisitions from the same crystal block on the SensL detector.

These resolvability index results suggest that one could expect to decode more crystals with multiplexed SensL SPM arrays, than we have attempted here. In our dual layer studies, there are only 25 crystals decoded with 16 sensors, so one would expect that the resolvability would be better than encoding 169 crystals with only four PMTs even though the noise in the SPM readout is greater than in conventional PMTs.

There is no significant difference between the spectral FWHM in the lower layer, but the upper layer is slightly worse. The difference in FWHM between the 16 channel and multiplexed acquisitions is barely significant. The spectra in Fig. 5 show the variability of the light collected from each

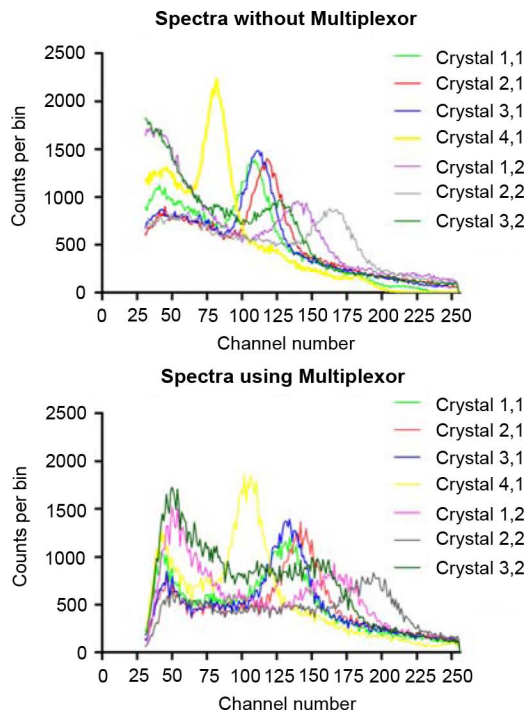


Fig. 5. Spectra from 7 crystals acquired with: Top: 16 channels; and Bottom: 16:3 multiplexed acquisition. The crystals numbered (n, 1) are in the layer nearer the PMT face, those numbered (n, 2) are in the far layer.

gains of the two processing chains are different the horizontal scale for these two figures is different. In all cases the 511 keV gamma ray peak is clearly visible. The energy resolution values are given in Table IV. The mean values for energy resolution degrade from 33.5% to 35.0% in the lower layer, and from 30.4 to 36.1% in the upper layer when the 16 channel acquisition is compared to the 16:3 MPX acquisition.

TABLE IV
ENERGY RESOLUTION FOR EACH OF THE CRYSTALS IN EACH ROW AND LAYER IN THE DUAL-LAYER BLOCK. BOTH 16 CHANNEL AND 16:3 MPX RESULTS ARE SHOWN

Crystal# Acquisition	Lower Layer					Upper Layer			
	1	2	3	4	Mean	1	2	3	Mean
Std Array: Energy Resolution (FWHM %)	35.3	36.6	32.9	29.1	33.5±3.2	37.5	29.6	24.0	30.4±3.9
MPX Array: Energy Resolution (FWHM %)	41.9	30.3	32.0	35.6	35.0±2.6	42.2	30.1	36.0	36.1±3.5

due to coupling, position and SPM gain. There is considerable variation, but no consistent difference between the lower ($y = 1$) and upper ($y = 2$) layers. One can see more bin-to-bin noise present in the 3-channel acquisition even though there are about the same number of counts in each spectrum. Comparing the spectrum of individual crystal elements in Fig. 5 for both acquisitions, the multiplexed one clearly has more bin-to-bin noise even though the counts per bin are about the same. This increase in noise thus cannot be explained by counting statistics. However if one considers that in the 16 channel acquisition there is always more than one ADC contributing to the assignment of a specific spectral bin for each event (and the rest of the channels are also contributing noise) this has the effect of making for a smoother spectrum, than when only one ADC is used to make the spectrum. This increased noise may be due to the differential non-linearity of the one single ADC to estimate the energy rather than an increase in statistical noise.

V. CONCLUSION

We have shown that a 16:3 multiplexor provides a realistic readout strategy for the SensL 4×4 SPM array coupled to crystal blocks which could be used in high resolution PET scanners. Reducing the number of readout channels from 16 to 3 provides a lower acquisition channel requirement than is used in current PET scanner practise, while providing comparable or better resolvability of the individual crystals. It is likely that these multiplexed arrays could be incorporated into conventional PET scanners to encode detector blocks with even more crystals providing improved spatial resolution in both pre-clinical and conventional whole body PET scanners.

ACKNOWLEDGMENT

The authors are grateful to Hank Shlosser of the Niagara Engineering Works Inc., Winnipeg, MB, Canada for the detailed multiplexor design, circuit layout, and construction (<http://www.NiagaraEngineeringWorks.Ca>). The authors appreciate the help and cooperation of Carl Jackson and John

Murphy of SensL Inc., Cork, Ireland enabling the authors' first use of their devices.

REFERENCES

- [1] R. Lecomte, D. Schmitt, A. W. Lightstone, and R. J. McIntyre, "Performance characteristics of BGO-silicon avalanche photodiode detectors for PET," *IEEE Trans. Nucl. Sci.*, vol. NS-32, no. 1, pp. 482–486, Feb. 1985.
- [2] B. Dolgoshein *et al.*, "Calice SiPM collaboration Status report on silicon photomultiplier development and applications," *Nucl. Instrum. Methods Phys. Res. A*, vol. 563, no. 2, pp. 366–376, 2006.
- [3] R. Grazioso *et al.*, "APD-based PET detector for simultaneous PET/MR imaging," *Nucl. Instrum. Methods Phys. Res. A*, vol. 569, no. 3, pp. 810–814, 2006.
- [4] M. E. Casey and R. Nutt, "A multi-crystal two dimensional BGO detector system for positron emission tomography," *IEEE Trans. Nucl. Sci.*, vol. NS-33, no. 1, pp. 460–463, Feb. 1986.
- [5] P. D. Olcott, H. Peng, and C. S. Levin, "Solid state photomultiplier (SSPM)-based PET detector with capacitively multiplexed readout and electro-optical coupling for PET/MR," *J. Nucl. Med.*, vol. 50, pp. 92–93, 2009.
- [6] C. J. Thompson, M.-L. Camborde, and M. E. Casey, "A central positron source to perform the timing alignment of detectors in a PET scanner," *IEEE Trans. Nucl. Sci.*, vol. 52, no. 5, pp. 1300–1304, Oct. 2005.
- [7] SensL Inc., Cork, Ireland [Online]. Available: <http://sensl.com/products/silicon-photomultipliers/spmarray4>
- [8] C. J. Thompson, "Effects on the gains and time delays of an array of SPMs due to changing bias voltage," in *Proc. IEEE Medical Imaging Conf. Rec.*, Knoxville, TN, Nov. 2010, pp. M14–48, CD-ROM.
- [9] W. H. Press, B. P. Flannery, S. A. Teukolsky, and W. T. Vetterling, *Numerical Recipes, The Art of Scientific Computing*. Cambridge, U.K.: Cambridge Univ. Press, 1988.
- [10] C. Pang, W. Lam, and N. Yung, "A method of vehicle count in the presence of multiple-vehicle occlusions in traffic images," *IEEE Trans. Intell. Transp. Syst.*, vol. 8, no. 3, pp. 441–459, 2007.
- [11] M. Brambilla, C. Secco, M. Dominiotto, R. Matheoud, G. Sacchetti, and E. Inglese, "Performance characteristics obtained for a new 3-dimensional lutetium oxy-orthosilicate based whole-body PET/CT scanner with the national electrical manufacturers association NU 2-2001 standard," *J. Nucl. Med.*, vol. 46, pp. 2083–91, 2005.
- [12] C. C. Constatinescu and J. Mukherjee, "Performance evaluation of an Inveon PET preclinical scanner," *Phys. Med. Biol.*, vol. 54, pp. 2885–2899, 2009.
- [13] GraphPad "Prism" version 5.03 for Windows, GraphPad Software, San Diego CA [Online]. Available: <http://www.graphpad.com>
- [14] C. J. Thompson, "Optimizing MRI-PET inserts for uniform spatial resolution and enhanced efficiency," presented at the IEEE Medical Imaging Conf., 2008, M6-49.